Optimal Placement of Phasor Measurement Unit in Smart Grids Considering Multiple Constraints

Tengpeng Chen, He Ren, Yuhao Sun, Markus Kraft, and Gehan A. J. Amaratunga

***Abstract*—The distribution of measurement noise is usually assumed to be Gaussian in the optimal phasor measurement unit (PMU) placement (OPP) problem. However, this is not always accurate in practice. This paper proposes a new OPP method for smart grids in which the effects of conventional measurements, limited channels of PMUs, zero-injection buses (ZIBs), single PMU loss contingency, state estimation error (SEE), and the maximum SEE variance (MSEEV) are considered. The SEE and MSEEV are both obtained using a robust *t*-distribution maximum likelihood estimator (MLE) because *t*-distribution is more flexible for modeling both Gaussian and non-Gaussian noises. The A- and G-optimal experimental criteria are utilized to form the SEE and MSEEV constraints. This allows the optimization problem to be converted into a linear objective function subject to linear matrix inequality observability constraints. The performance of the proposed OPP method is verified by the simulations of the IEEE 14-bus, 30-bus, and 118-bus systems as well as the 211-bus practical distribution system in China.**

***Index Terms*—Phasor measurement unit (PMU), smart grids, optimal placement, state estimation (SE).**

I. Introduction

STATE estimation (SE) is essential in smart grids because it can provide real-time SE variables to the control center of the power system to achieve high operational reliability and safety [1], [2]. The data used for SE are normally obtained from a supervisory control and data acquisition (SCADA) system. In the last decade, phasor measurement units (PMUs), which use a global positioning system (GPS) signal in a power system, have been developed. This has resulted in the availability of measurements with higher accuracies [3], [4]. Therefore, the accuracy of SE variables can be further improved if more PMUs are installed to increase the number of accurate measurements in smart grids [5].

However, PMU installation costs remain high, making it infeasible to install PMUs on all buses in a power system [6]. Therefore, optimal PMU placement (OPP) has become a requirement and a subject of active research. The objective of the traditional OPP problem is to minimize the number of PMUs while making the entire power system completely observable [7]. However, it has been proven that the minimum number of installed PMUs will not be translated into the lowest cost for synchrophasor deployment [8]-[11]. For example, the formulation of the OPP problem needs to consider the numbers of devices and substations that must be upgraded to support these devices simultaneously [10]. Moreover, many OPP methods that use different objective functions and practical constraints have been proposed for transmission systems [12]-[15] and distribution systems [7], [16]-[19]. For example, a multi-objective OPP method that simultaneously considers the small-signal stability of the power system, the probability of system observability, and the total cost of PMUs is proposed in [12]. The OPP problem for the co-optimal placement of PMUs and their communication infrastructure for the minimization of the propagation delay in a monitoring system is presented in [20]. The optimal PMU communication link placement problem that investigates the placement of PMUs and communication links for full observability in a power system is presented in [13]. The OPP problem considering the channel limits (CLs) and PMU loss contingency is presented in [14]. An efficient method for the placement of traditional nonsynchronized measurements and synchronized measurements using a Boolean semidefinite programming (SDP) approach and the number of available channels is considered in [21]. An OPP problem that considers both the communication infrastructure and the installation cost of PMUs is presented in [22]. An OPP framework that considers both the installation cost of PMUs and the observability that incorporates network vulnerabilities as the objective is discussed in [23]. The effects of zero-injection buses (ZIBs) on the optimization problem for reducing the number of PMUs are considered in [16]. In all of the proposed methods, the OPP solution plays an essential role in the design of the wide-area measurement system (WAMS) and ulti-

Manuscript received: January 6, 2022; revised: April 25, 2022; accepted: July 12, 2022. Date of CrossCheck: July 12, 2022. Date of online publication: July 22, 2022.

This work was supported by the National Natural Science Foundation of China (No. 61903314), Basic Research Program of Science and Technology of Shenzhen, China (No. JCYJ20190809162807421), Natural Science Foundation of Fujian Province (No. 2019J05020), and National Research Foundation, Prime Minister's Office, Singapore under its Campus for Research Excellence and Technological Enterprise (CREATE) programme.

T. Chen (corresponding author) and H. Ren are with the Department of Instrumental and Electrical Engineering, Xiamen University, Xiamen, China, and T. Chen is also with the Shenzhen Research Institute of Xiamen University, Shenzhen, China (e-mail: tpchen@xmu.edu.cn; 35120191151214@stu.xmu.edu.cn).

Y. Sun is with CTC Intelligence (Shenzhen) Technology Co., Ltd., Shenzhen, China (e-mail: ysun@ctcintelli.com).

M. Kraft is with the Department of Chemical Engineering and Biotechnology, University of Cambridge, Cambridge, UK, the Cambridge Centre for Advanced Research and Education in Singapore, CREATE Tower, Singapore, and he is also with School of Chemical and Biomedical Engineering, Nanyang Technological University, Singapore (e-mail: mk306@cam.ac.uk).

G. A. J. Amaratunga is with the Department of Engineering, University of Cambridge, UK (e-mail: ga@eng.cam.ac.uk).

DOI: 10.35833/MPCE.2022.000003

mately influences the SE accuracy of the power system. A WAMS is widely applied in smart grids [5]. Therefore, OPP and SE should work together. However, in the above OPP methods, the state estimation error (SEE) is not integrated into the optimization problem and is therefore an unknown quantity.

Since the same OPP problem may have multiple solutions and these solutions have the same system observability redundancy index, [24] takes the trace of the SEE variance as a new index so that the final solution can be obtained. The OPP problem of minimizing the mean squared error by incorporating various constraints such as ZIBs, the contingency of the measurement loss, and the limitations of communication channels is investigated in [25]. A measurement allocation method for the distribution system, in which the maximum SEE variance (MSEEV) is taken as the minimum objective function, is proposed in [7]. On the basis of the optimal experimental criteria, four indices related to the SEE variance matrix are utilized in [26], and a meter selection method is presented to choose certain measurements from a set of candidate measurements. A formulation of the OPP problem for minimizing the uncertainty in SE in distribution networks is reported in [18]. A shortcoming of the above methods is that the considered SEE is based on the weighted least-squares (WLS) estimator, and the measurement noise is assumed to be Gaussian. However, [27] and [28] find that the distribution of PMU measurement noise is non-Gaussian. Therefore, the previous work in [29], [30] introduces an optimal PMU selection method, in which the measurement noise is considered as non-Gaussian and the maximum likelihood estimator (MLE) is applied. However, this method is one kind of PMU selection methods and is based on the assumption that a sufficient number of PMUs are installed in the monitoring system. In addition, the objective function applied in [29] is time-consuming and cannot be guaranteed to obtain the minimum sum of variances. Moreover, the effects of the PMU CLs, ZIBs, PMU loss contingency, and MSEEV are not considered. The approximate solution method presented in [26], [29] cannot easily obtain OPP solutions, particularly when the dimension of the optimization problem is large. Even though [14] proposes an efficient algorithm to obtain the minimum number of PMUs, where various constraints such as PMU CLs, ZIBs, and PMU loss contingency are considered, it does not consider the SEE and MSEEV in the OPP problem.

This paper presents a new OPP method for smart grids, where PMU CLs, ZIBs, single PMU loss contingency, SCADA measurements, SEE, and MSEEV are considered. Considering that the A- and G-optimal experimental criteria are based on the gain matrix of the WLS method and that the WLS estimator is usually based on the assumption of Gaussian noise, an approximate matrix is derived to represent the gain matrix of a robust estimator. The form of the approximate matrix is similar to the gain matrix of the WLS method so that the derived approximate matrix can still be applied in the above experimental design criteria. A comparison of representative OPP methods and the proposed OPP method is summarized in Table I, where √ and × represent the method with and without this scenario capability, respectively.

TABLE I
COMPARISON OF REPRESENTATIVE OPP METHODS AND PROPOSED METHOD

Method	SCADA measurement	Robust estimator	SEE & Gaussian noise	MSEEV & Gaussian noise	SEE & non-Gaussian noise	MSEEV & non-Gaussian noise	ZIB	CL	Single PMU loss contingency
[7]	√	×	×	√	×	×	×	×	×
[26]	√	×	√	√	×	×	×	×	×
[19]	√	×	√	×	×	×	×	×	×
[29]	√	√	×	×	√	√	×	×	×
[30]	×	√	×	×	√	√	×	×	×
Proposed method	√	√	√	√	√	√	√	√	√

The main contributions of this study are summarized as follows.

1) A new OPP method considering PMU CLs, ZIBs, single PMU loss contingency, SCADA measurements, SEE, and MSEEV is proposed.

2) The considered SEE and MSEEV constraints are calculated on the basis of the *t*-distribution model and are formulated as linear matrix inequality observability constraints.

3) The proposed OPP method is also useful for designing or upgrading WAMSs.

For simplicity, only the MLE is considered in the optimization problem. However, the proposed OPP method can also be based on other robust estimators presented in [31], [32].

The remainder of this paper is structured as follows. The SE problem is formulated in Section II. A new OPP method that considers multiple constraints is presented in Section III. The performance of the proposed OPP method is evaluated in Section IV. Finally, the conclusions are presented in Section V.

II. SE PROBLEM FORMULATION

Rectangular coordinates are used to present the measurements and system states. The linear measurement model is given by (1) if PMUs are used [31].

$$\boldsymbol{z}=\boldsymbol{H}\boldsymbol{x}+\boldsymbol{\epsilon} \tag{1}$$

where $\boldsymbol{z}=[z_1,z_2,\ldots,z_m]^{\mathrm{T}}$ is the measurement vector that includes the bus voltage phasors and branch current phasors [33]; $\boldsymbol{x}=[E_1^{re},E_2^{re},\ldots,E_{n/2}^{re},E_1^{im},E_2^{im},\ldots,E_{n/2}^{im}]^{\mathrm{T}}$ is the vector of

the system state variables consisting of the real and imaginary parts of the bus voltage phasors; $\boldsymbol{H}=[\boldsymbol{H}_1^{\mathrm{T}},\boldsymbol{H}_2^{\mathrm{T}},\ldots,\boldsymbol{H}_m^{\mathrm{T}}]^{\mathrm{T}}$ is the measurement matrix with the dimension of $m\times n$, which is calculated according to the topology of the power system and the locations of PMUs; and $\boldsymbol{\epsilon}=[\epsilon_1,\epsilon_2,\ldots,\epsilon_m]^{\mathrm{T}}$ is the noise vector. The measurement residual $\boldsymbol{e}$ is formulated as:

$$\boldsymbol{e}=\boldsymbol{z}-\boldsymbol{H}\hat{\boldsymbol{x}} \tag{2}$$

where $\hat{\boldsymbol{x}}$ is the estimated state vector; and $\boldsymbol{e}=[e_1,e_2,\ldots,e_m]^{\mathrm{T}}$.

The well-known WLS, a non-robust estimator, is based on the assumption of Gaussian measurement noise. Considering that the distribution of the PMU measurement noise is non-Gaussian [27], the SEE presented in this paper is calculated using the MLE presented in [34]. The *t*-distribution is given as:

$$f_i(\epsilon_i)=\frac{\Gamma\left(\frac{v_i+1}{2}\right)}{\sqrt{v_i\pi}\,\xi_i\Gamma\left(\frac{v_i}{2}\right)}\left(1+\frac{|\epsilon_i|^2}{\xi_i^2 v_i}\right)^{-\frac{v_i+1}{2}} \tag{3}$$

where $\Gamma(\cdot)$ is the Gamma function; ξ_i is the scale parameter; and v_i is the shape parameter. A *t*-distribution with a "heavy tail" is suitable for characterizing Gaussian or non-Gaussian noise [34], [35].

The MLE can be implemented by minimizing [34]:

$$J=-\sum_{i=1}^{m}\ln(f_i(e_i)) \tag{4}$$

Differentiating J with respect to $\hat{\boldsymbol{x}}$ yields (5), since $\partial e_i/\partial\hat{\boldsymbol{x}}=-\boldsymbol{H}_i^{\mathrm{T}}$.

$$\boldsymbol{\Psi}=\frac{\partial J}{\partial e_i}\frac{\partial e_i}{\partial\hat{\boldsymbol{x}}}=-\sum_{i=1}^{m}\frac{\partial\ln(f_i(e_i))}{\partial e_i}\frac{1}{e_i}e_i\frac{\partial e_i}{\partial\hat{\boldsymbol{x}}}=-\sum_{i=1}^{m}W_i e_i\boldsymbol{H}_i^{\mathrm{T}}=-\boldsymbol{H}^{\mathrm{T}}\boldsymbol{W}\boldsymbol{e} \tag{5}$$

where $\boldsymbol{W}=\mathrm{diag}(W_1,W_2,\ldots,W_m)$ is a diagonal matrix, in which W_i is given as:

$$W_i=\frac{\partial\ln f_i(e_i)}{\partial e_i}\frac{1}{e_i}=\frac{v_i+1}{\xi_i^2 v_i+e_i^2} \tag{6}$$

Setting $\boldsymbol{\Psi}=\boldsymbol{0}$, the estimate from the MLE is given as:

$$\hat{\boldsymbol{x}}=(\boldsymbol{H}^{\mathrm{T}}\boldsymbol{W}\boldsymbol{H})^{-1}\boldsymbol{H}^{\mathrm{T}}\boldsymbol{W}\boldsymbol{z} \tag{7}$$

Using (2), the iteration form (8) is used to obtain a more precise estimate.

$$\hat{\boldsymbol{x}}^k=\hat{\boldsymbol{x}}^{k-1}+(\boldsymbol{H}^{\mathrm{T}}\boldsymbol{W}^{k-1}\boldsymbol{H})^{-1}\boldsymbol{H}^{\mathrm{T}}\boldsymbol{W}^{k-1}\boldsymbol{e}^{k-1} \tag{8}$$

where k is the iteration step. Iteration stops when $\hat{\boldsymbol{x}}^k-\hat{\boldsymbol{x}}^{k-1}$ is less than a predetermined value.

III. Proposed OPP Method

On the basis of the optimization problem in [30], the objective of the proposed OPP method is to obtain the minimum number of PMUs while considering the PMU CLs, ZIBs, single PMU loss contingency, SCADA measurements, SEE, and MSEEV.

A. Preliminaries of Proposed OPP Method

According to spectral graph theory, $V=\{1,2,\ldots,b\}$ represents the set of buses of the entire power system, and $b=|V|$ is the number of buses. If the PMU CLs are not considered, the decision vector for PMU placement is given as:

$$\boldsymbol{p}=[p_1\quad p_2\quad\cdots\quad p_b]^{\mathrm{T}}\in\mathbb{R}^{b\times 1} \tag{9}$$

where p_j is a binary variable given as:

$$p_j=\begin{cases}1 & \text{one PMU is placed at bus } j\\ 0 & \text{otherwise}\end{cases} \tag{10}$$

In order to discuss numerical observability, a new measurement matrix is defined as:

$$\bar{\boldsymbol{H}}=[\bar{\boldsymbol{H}}_1^{\mathrm{T}}\quad\bar{\boldsymbol{H}}_2^{\mathrm{T}}\quad\cdots\quad\bar{\boldsymbol{H}}_b^{\mathrm{T}}]^{\mathrm{T}} \tag{11}$$

where $\bar{\boldsymbol{H}}_j$ is the measurement submatrix associated with a PMU installed at bus j.

By selecting the WLS method with the Gaussian noise assumption, the SEE variance matrix can be represented by [32]:

$$\boldsymbol{\Phi}_W=\left(\sum_{j\in V}\bar{\boldsymbol{H}}_j^{\mathrm{T}}\bar{R}_j^{-1}\bar{\boldsymbol{H}}_j\right)^{-1} \tag{12}$$

where $\bar{R}_j=\sigma_j^2$ is the element of a diagonal matrix $\bar{\boldsymbol{R}}$, and σ_j is the standard deviation of the j^{th} Gaussian measurement noise. The premise of (12) is that there are a sufficient number of PMUs installed on certain buses, which makes the entire power system observable, and $\sum_{j\in V}\bar{\boldsymbol{H}}_j^{\mathrm{T}}\bar{R}_j^{-1}\bar{\boldsymbol{H}}_j$ has full rank $\left(\sum_{j\in V}\bar{\boldsymbol{H}}_j^{\mathrm{T}}\bar{R}_j^{-1}\bar{\boldsymbol{H}}_j\succ 0\right)$.

When other robust estimators are applied in the case of non-Gaussian measurement noise, $\boldsymbol{\Phi}_W$ can no longer be used to calculate the SEE variance matrix. Thus, we define (13) to further derive the SEE and MSEEV of the robust estimators in the case of non-Gaussian noise.

$$\boldsymbol{\Phi}_R=\left(\sum_{j\in V}\bar{\boldsymbol{H}}_j^{\mathrm{T}}\bar{\boldsymbol{\Pi}}_j\bar{\boldsymbol{H}}_j\right)^{-1} \tag{13}$$

where $\bar{\boldsymbol{\Pi}}_j$ is a diagonal matrix under non-Gaussian measurement noise.

The influence function (IF) can be further used to derive the SEE variance matrix of an estimator [30], [36], [37]:

$$\boldsymbol{\Phi}_V=\left(\int_{-\infty}^{\infty}\frac{\partial\boldsymbol{\Psi}(\boldsymbol{\epsilon})}{\partial\hat{\boldsymbol{x}}}\mathrm{d}F(\boldsymbol{\epsilon})\right)^{-1}\int_{-\infty}^{\infty}\boldsymbol{\Psi}(\boldsymbol{\epsilon})(\boldsymbol{\Psi}(\boldsymbol{\epsilon}))^{\mathrm{T}}\mathrm{d}F(\boldsymbol{\epsilon})\cdot\left(\left(\int_{-\infty}^{\infty}\frac{\partial\boldsymbol{\Psi}(\boldsymbol{\epsilon})}{\partial\hat{\boldsymbol{x}}}\mathrm{d}F(\boldsymbol{\epsilon})\right)^{-1}\right)^{\mathrm{T}} \tag{14}$$

where $F(\boldsymbol{\epsilon})$ is the joint distribution; and $\mathrm{d}F(\boldsymbol{\epsilon})$ is given as:

$$\mathrm{d}F(\boldsymbol{\epsilon})=f_1(\epsilon_1)f_2(\epsilon_2)\cdot\ldots\cdot f_m(\epsilon_m)\mathrm{d}\epsilon_1\mathrm{d}\epsilon_2\cdot\ldots\cdot\mathrm{d}\epsilon_m \tag{15}$$

From the differentiation in (5), (14) can be expressed as:

$$\boldsymbol{\Phi}_V=(\bar{\boldsymbol{H}}^{\mathrm{T}}\bar{\boldsymbol{U}}\bar{\boldsymbol{H}})^{-1}(\bar{\boldsymbol{H}}^{\mathrm{T}}\bar{\boldsymbol{S}}\bar{\boldsymbol{H}})((\bar{\boldsymbol{H}}^{\mathrm{T}}\bar{\boldsymbol{U}}\bar{\boldsymbol{H}})^{-1})^{\mathrm{T}}=\left(\bar{\boldsymbol{H}}^{\mathrm{T}}\int_{-\infty}^{\infty}\frac{\partial\boldsymbol{W}\boldsymbol{\epsilon}}{\partial\boldsymbol{\epsilon}}\mathrm{d}F(\boldsymbol{\epsilon})\bar{\boldsymbol{H}}\right)^{-1}\left(\bar{\boldsymbol{H}}^{\mathrm{T}}\int_{-\infty}^{\infty}\boldsymbol{W}\boldsymbol{\epsilon}\boldsymbol{\epsilon}^{\mathrm{T}}\boldsymbol{W}^{\mathrm{T}}\mathrm{d}F(\boldsymbol{\epsilon})\bar{\boldsymbol{H}}\right)\cdot\left(\left(\bar{\boldsymbol{H}}^{\mathrm{T}}\int_{-\infty}^{\infty}\frac{\partial\boldsymbol{W}\boldsymbol{\epsilon}}{\partial\boldsymbol{\epsilon}}\mathrm{d}F(\boldsymbol{\epsilon})\bar{\boldsymbol{H}}\right)^{-1}\right)^{\mathrm{T}} \tag{16}$$

where $\bar{\boldsymbol{U}}$ and $\bar{\boldsymbol{S}}$ are the diagonal matrices, which are given as (17) and (18), and and their elements are formulated as (19) and (20), respectively.

$$\bar{\boldsymbol{U}}=\int_{-\infty}^{\infty}\frac{\partial \boldsymbol{W}\boldsymbol{\epsilon}}{\partial \boldsymbol{\epsilon}}\mathrm{d}F(\boldsymbol{\epsilon}) \tag{17}$$

$$\bar{\boldsymbol{S}}=\int_{-\infty}^{\infty}\boldsymbol{W}\boldsymbol{\epsilon}\boldsymbol{\epsilon}^{\mathrm{T}}\boldsymbol{W}^{\mathrm{T}}\mathrm{d}F(\epsilon) \tag{18}$$

$$\bar{U}_i=\int_{-\infty}^{\infty}\frac{(v_i+1)(\xi_i^{\ 2}v_i-\epsilon_i^2)}{(\xi_i^{\ 2}v_i+\epsilon_i^2)^2}f_i(\epsilon_i)\mathrm{d}\epsilon_i \tag{19}$$

$$\bar{S}_i=\int_{-\infty}^{\infty}\frac{(v_i+1)^2\epsilon_i^2}{(\xi_i^{\ 2}v_i+\epsilon_i^2)^2}f_i(\epsilon_i)\mathrm{d}\epsilon_i \tag{20}$$

B. Link Between MLE and WLS

Considering that (13) and (16) are symmetric matrices, (13) is used to approximate (16). Therefore, the structure of the approximate gain matrix is identical to that of the gain matrix of the WLS method:

$$(\bar{\boldsymbol{H}}^{\mathrm{T}}\bar{\boldsymbol{\Pi}}\bar{\boldsymbol{H}})^{-1}\approx(\bar{\boldsymbol{H}}^{\mathrm{T}}\bar{\boldsymbol{U}}\bar{\boldsymbol{H}})^{-1}(\bar{\boldsymbol{H}}^{\mathrm{T}}\bar{\boldsymbol{S}}\bar{\boldsymbol{H}})((\bar{\boldsymbol{H}}^{T}\bar{\boldsymbol{U}}\bar{\boldsymbol{H}})^{-1})^{\mathrm{T}} \tag{21}$$

where $\bar{\boldsymbol{\Pi}}$ is an approximate matrix.

According to [35], the t-distribution in (3) with $v_i\to\infty$ and $\xi_i=\sigma_i$ reduces to a Gaussian distribution. Equations (19) and (20) then become

$$\bar{U}_i=\lim_{v_i\to\infty,\xi_i=\sigma_i}\int_{-\infty}^{+\infty}\frac{(v_i+1)(\xi_i^2v_i-\epsilon_i^2)}{(\xi_i^2v_i+\epsilon_i^2)^2}f_i(\epsilon_i)\mathrm{d}\epsilon_i=\bar{R}_i^{-1} \tag{22}$$

$$\bar{S}_i=\lim_{v_i\to\infty,\xi_i=\sigma_i}\int_{-\infty}^{\infty}\frac{(v_i+1)^2\epsilon_i^2}{(\xi_i^2v_i+\epsilon_i^2)^2}f_i(\epsilon_i)\mathrm{d}\epsilon_i=\bar{R}_i^{-1} \tag{23}$$

where $\bar{R}_i=\sigma_i^2$.

In this case, (21) can be rewritten as:

$$\boldsymbol{\Phi}_{R'}=(\bar{\boldsymbol{H}}^{\mathrm{T}}\bar{\boldsymbol{R}}^{-1}\bar{\boldsymbol{H}})^{-1}(\bar{\boldsymbol{H}}^{\mathrm{T}}\bar{\boldsymbol{R}}^{-1}\bar{\boldsymbol{H}})((\bar{\boldsymbol{H}}^{\mathrm{T}}\bar{\boldsymbol{R}}^{-1}\bar{\boldsymbol{H}})^{-1})^{\mathrm{T}}=(\bar{\boldsymbol{H}}^{\mathrm{T}}\bar{\boldsymbol{R}}^{-1}\bar{\boldsymbol{H}})^{-1} \tag{24}$$

This demonstrates that the utilized t-distribution-based MLE can also be used to represent the WLS estimator under the assumption of Gaussian noise.

C. OPP Problem Considering PMU CLs, ZIBs, Single PMU Loss Contingency, SEE, and MSEEV

A key contribution of this study is linking OPP and SE of the power system. The SEE and MSEEV constraints can be represented as linear matrix inequality constraints using A- and G-optimal experimental criteria. Note that the A-optimal experimental criterion is equivalent to minimizing the mean of the norm of the squared error when estimating the state variables, and the associated objective is to minimize the average variance [26]:

$$J_A(\boldsymbol{p})=trace\left(\sum_{j\in V}p_j\bar{\boldsymbol{H}}_j^{\mathrm{T}}\bar{\boldsymbol{\Pi}}_j\bar{\boldsymbol{H}}_j\right)^{-1} \tag{25}$$

where *trace*(·) is the trace or sum of the diagonal elements of the matrix. The SEE is expressed by $trace\left(\sum_{j\in V}p_j\bar{\boldsymbol{H}}_j^{\mathrm{T}}\bar{\boldsymbol{\Pi}}_j\bar{\boldsymbol{H}}_j\right)^{-1}$ given in (25). The error variance matrix $\left(\sum_{j\in V}p_j\bar{\boldsymbol{H}}_j^{\mathrm{T}}\bar{\boldsymbol{\Pi}}_j\bar{\boldsymbol{H}}_j\right)^{-1}$ represents the corresponding SE accuracy and provides a quantitative measure of how informative the placement of the b PMUs is. Each PMU j is characterized by its measurement submatrix $\bar{\boldsymbol{H}}_j$. The G-optimal experimental criterion is equivalent to minimizing the largest diagonal entry of the error variance matrix [7]:

$$J_G(\boldsymbol{p})=\max_{r=1,2,\ldots,n}\left[\left(\sum_{j\in V}p_j\bar{\boldsymbol{H}}_j^{\mathrm{T}}\bar{\boldsymbol{\Pi}}_j\bar{\boldsymbol{H}}_j\right)^{-1}\right]_r \tag{26}$$

Note that the A-optimal experimental criterion minimizes the total variance of the state estimates, and the G-optimal experimental criterion minimizes the worst possible variance among state estimates. In this study, the total variance of the state estimates and the worst possible variance are considered in the optimization problem. The MSEEV is expressed by the maximum element of the matrix $\left(\sum_{j\in V}p_j\bar{\boldsymbol{H}}_j^{\mathrm{T}}\bar{\boldsymbol{\Pi}}_j\bar{\boldsymbol{H}}_j\right)^{-1}$ in (26).

According to [26], [30], defining $\boldsymbol{\chi}=[\chi_1,\chi_2,\ldots,\chi_n]^{\mathrm{T}}$, in which χ_r is the largest diagonal element of the matrix $\left[\left(\sum_{j\in V}p_j\bar{\boldsymbol{H}}_j^{\mathrm{T}}\bar{\boldsymbol{\Pi}}_j\bar{\boldsymbol{H}}_j\right)^{-1}\right]_r$, there exists

$$\chi_r-\boldsymbol{e}_r^{\mathrm{T}}\left(\sum_{j\in V}p_j\bar{\boldsymbol{H}}_j^{\mathrm{T}}\bar{\boldsymbol{\Pi}}_j\bar{\boldsymbol{H}}_j\right)^{-1}\boldsymbol{e}_r\geq 0\quad r=1,2,\ldots,n \tag{27}$$

where $\boldsymbol{e}_r$ is the placement decision vector with 1 for the r^{th} entry and 0 for the remaining elements. Thus, (27) can be rewritten as (28) to represent the matrix $\sum_{j\in V}p_j\bar{\boldsymbol{H}}_j^{\mathrm{T}}\bar{\boldsymbol{\Pi}}_j\bar{\boldsymbol{H}}_j$, which has full rank [38].

$$\begin{bmatrix}\sum_{j\in V}p_j\bar{\boldsymbol{H}}_j^{\mathrm{T}}\bar{\boldsymbol{\Pi}}_j\bar{\boldsymbol{H}}_j & \boldsymbol{e}_r\\ \boldsymbol{e}_r^{\mathrm{T}} & \chi_r\end{bmatrix}\succ 0\quad r=1,2,\ldots,n \tag{28}$$

Note that the premise of (25) and (26) is to make the matrix $\sum_{j\in V}p_j\bar{\boldsymbol{H}}_j^{\mathrm{T}}\bar{\boldsymbol{\Pi}}_j\bar{\boldsymbol{H}}_j$ full rank.

In addition, voltage channels are always available, and the number of branch current channels is limited according to [14]. We define d_j and ι as the number of branches connected to bus j and the number of available PMU channels, respectively. We define C_j as the set of all possible combinations of $d_j!/\iota!/(d_j-\iota)!$ at bus j. The vector $[q_{j,0},q_{j,1},\ldots,q_{j,d_j}]^{\mathrm{T}}$ is the placement decision subvector related to the voltage phasor and branch current phasor measurements connected to bus j. Therefore, the new placement decision vector considering the CLs is given as:

$$\boldsymbol{q}=[q_{1,0}\quad q_{1,1}\quad\cdots\quad q_{1,d_1}\quad\cdots\quad q_{b,0}\quad q_{b,1}\quad\cdots\quad q_{b,d_b}]^{\mathrm{T}} \tag{29}$$

where $q_{j,0}$ is the decision variable associated with the voltage phasor at bus j; and $q_{j,g}(g\geq 1)$ is the decision variable that is related to the branch current phasor measurements and is a binary variable given as follows:

$$q_{j,g}=\begin{cases}1 & \text{if } q_{j,0}=1 \text{ and the } g^{\mathrm{th}} \text{ channel of PMU}\\ & \text{placed at bus } j \text{ is available}\\ 0 & \text{otherwise}\end{cases} \tag{30}$$

The dimension of the new PMU placement decision vector $\boldsymbol{q}$ is given as:

$$\lambda = b + d_1 + d_2 + \ldots + d_b \tag{31}$$

The placement decision vector $\boldsymbol{p}$ without considering CLs is expressed as to (32) because the decision vector related to the current phasor measurements is set as $q_{j,g} = q_{j,0}$ by default if the PMU CLs are not considered.

$$\boldsymbol{p} = [p_1 \quad p_2 \quad \cdots \quad p_b]^{\mathrm{T}} = [q_{1,0} \quad q_{2,0} \quad \cdots \quad q_{b,0}]^{\mathrm{T}} \tag{32}$$

According to (29) and (32), it is clear that the dimension of the problem given in (33) is larger than that presented in [30]. The ZIBs, single PMU loss contingency, and existing SCADA measurements are widely considered in OPP problems [14], [39], [40]. The single PMU loss contingency means that any PMU may be lost. Thus, $V - \{j\}$ represents the set of remaining PMUs after the PMU installed at bus j is not available and $j \in V$. On the basis of [30], the OPP problem considering the PMU CLs, ZIBs, single PMU loss contingency, SEE, and MSEEV is formulated as a mixed-integer SDP (MISDP) problem:

$$\min \sum_{j \in V} \sum_{l \in C_j} q_{j,l} \tag{33}$$

s.t.

$$\boldsymbol{\Phi}_r \succ 0 \quad r = 1, 2, \ldots, n \tag{34}$$

$$C_j = d_j!/\iota!/(d_j - \iota)! \tag{35}$$

$$\sum_{r=1}^{n} \chi_r \le \delta_t \tag{36}$$

$$\max_{r=1,2,\ldots,n} \chi_r \le \delta_m \tag{37}$$

$$q_{j,l} \in \{0, 1\} \quad \forall j \in V, \forall l \in C_j \tag{38}$$

where δ_t and δ_m are the predetermined SEE and MSEEV tolerances, respectively. Note that the improper placement of PMUs would lead to a large SEE. The main motivation of this study is to link the PMU placement problem and SE accuracy and to find the OPP solution where the SEE is within a certain range. The proposed OPP problem is formulated according to [7], [14], [19], [26]. However, the MISDP problem presented in this paper is based on non-Gaussian noise and the MLE, whereas the MISDP model introduced in [7], [14], [19], [26] is formulated on the basis of Gaussian noise and the WLS estimator. Moreover, the proposed method links OPP and SEE of the power system; then, the SEE and MSEEV are taken as two key constraints that are not considered in [7], [14], [19], [26].

The measurement matrix $\bar{\boldsymbol{H}}_{j,l}$ is a subset of $\bar{\boldsymbol{H}}_j$ due to the PMU CLs. The matrix $\boldsymbol{\Phi}_r$ in (34) is given as:

$$\boldsymbol{\Phi}_r = \begin{bmatrix} \bar{\boldsymbol{\Gamma}} + \sum_{i \in V - \{j\}} \sum_{l \in C_j} q_{i,l} \bar{\boldsymbol{H}}_{i,l}^{\mathrm{T}} \bar{\boldsymbol{\Pi}}_{i,l} \bar{\boldsymbol{H}}_{i,l} & \boldsymbol{e}_r \\ \boldsymbol{e}_r^{\mathrm{T}} & \chi_r \end{bmatrix} \tag{39}$$

$$\bar{\boldsymbol{\Gamma}} = \tilde{\boldsymbol{H}}^{\mathrm{T}} \tilde{\boldsymbol{Y}} \tilde{\boldsymbol{H}} + \hat{\boldsymbol{H}}^{\mathrm{T}} \hat{\boldsymbol{Y}} \hat{\boldsymbol{H}} \tag{40}$$

The terms $\tilde{\boldsymbol{H}}^{\mathrm{T}} \tilde{\boldsymbol{Y}} \tilde{\boldsymbol{H}}$ and $\hat{\boldsymbol{H}}^{\mathrm{T}} \hat{\boldsymbol{Y}} \hat{\boldsymbol{H}}$ represent the effects of the ZIBs and pre-existing conventional measurements, respectively. For the optimization problem given in (33), in addition to the SEE and MSEEV constraints, the additional effects of the SCADA measurements ($\hat{\boldsymbol{Y}}$) and ZIBs ($\tilde{\boldsymbol{Y}}$) are considered. Note that PMU measurements are typically obtained at 30 or 60 samples per second, whereas the SCADA system can only obtain nonsynchronized measurements once every 2-4 s [37], [41]-[43]. The state estimates are usually updated slowly, once every few minutes [41] or several seconds (larger than the sampling period of the SCADA system), to reduce the computational complexity required to implement static SE. The variations in the system state variables within several consecutive measurement scans are negligible [44], and it can be assumed that the system state variables are constant during this interval [41]. Thus, the time stamp is not sensitive to static SE. The proposed OPP method is based on a static SE model and does not require time-stamping.

Different values of $\hat{\boldsymbol{Y}}$, $\tilde{\boldsymbol{Y}}$, and $\bar{\boldsymbol{\Pi}}$ would also lead to different solutions. According to [14], [32], [45], the conventional measurements utilized in this study include the injected power and power flow. Consider a π-model for the grid branch connecting buses i and j. The series admittance of branch ij is defined as $g_{ij} + \mathrm{j}y_{ij}$. The shunt admittance at bus i is defined as $g_{sij} + \mathrm{j}y_{sij}$. N_i represents the set of buses connected to bus i. ϵ_{P_i}, ϵ_{Q_i} and $\epsilon_{P_{ij}}$, $\epsilon_{Q_{ij}}$ represent the injected power and power flow measurement noises, respectively. The conventional measurements of the real and reactive power (or zero) injected at bus i can be written in a rectangular form as follows:

$$P_i = ((E_i^{re})^2 + (E_i^{im})^2) \sum_{j \in N_i} (g_{sij} + g_{ij}) + E_i^{re} \sum_{j \in N_i} (-g_{ij} E_j^{re} + y_{ij} E_j^{im}) - E_i^{im} \sum_{j \in N_i} (y_{ij} E_j^{re} + g_{ij} E_j^{im}) + \epsilon_{P_i} \tag{41}$$

$$Q_i = -((E_i^{re})^2 + (E_i^{im})^2) \sum_{j \in N_i} (y_{sij} + y_{ij}) + E_i^{re} \sum_{j \in N_i} (y_{ij} E_j^{re} + g_{ij} E_j^{im}) + E_i^{im} \sum_{j \in N_i} (-g_{ij} E_j^{re} + y_{ij} E_j^{im}) + \epsilon_{Q_i} \tag{42}$$

Note that for ZIB i, $P_i = Q_i = 0$. When the impact of ZIBs on SE is considered, the zero-injection power measurements and the corresponding linearized measurement matrix $\tilde{\boldsymbol{H}}$ derived from (41) and (42) should be included in (8). The measurements of the real and reactive power flows from bus i to bus j are given as:

$$P_{ij} = (g_{sij} + g_{ij})((E_i^{re})^2 + (E_i^{im})^2) + E_i^{re}(-g_{ij} E_j^{re} + y_{ij} E_j^{im}) - E_j^{im}(y_{ij} E_j^{re} + g_{ij} E_j^{im}) + \epsilon_{P_{ij}} \tag{43}$$

$$Q_{ij} = -(y_{sij} + y_{ij})((E_i^{re})^2 + (E_i^{im})^2) + E_i^{re}(y_{ij} E_j^{re} + g_{ij} E_j^{im}) + E_j^{im}(-g_{ij} E_j^{re} + y_{ij} E_j^{im}) + \epsilon_{Q_{ij}} \tag{44}$$

Therefore, the elements of the Jacobian matrices $\tilde{\boldsymbol{H}}$ and $\hat{\boldsymbol{H}}$ corresponding to measurements of the real and reactive injected power (or power flows) can be derived according to (41)-(44). More details can be found in [14].

D. Solution Method

Even though [26] and [29] provide a convex relaxation method to solve the MISDP problem, this method is not suitable for solving the proposed OPP problem given in (33). The main reasons are that many constraints are considered and the dimension of the PMU placement decision vector is increased. Following the method presented in [26], the methods for selecting the w largest elements of the suboptimal

placement solution p^* to be 1 cannot guarantee that a suboptimal solution of (33) can be obtained. This means that the suboptimal placement solution p^* is challenging to determine at the first step and the following approximate optimization step cannot be carried out. In this paper, the solutions of the proposed OPP problem can be obtained by directly using YALMIP with a CUTSDP solver [46] in MATLAB.

The procedure for solving the proposed OPP problem subject to different constraints is shown in Fig. 1. Note that the PMU installation costs include the specific cost of the PMU devices and other costs such as the cost of the communication infrastructure [6].

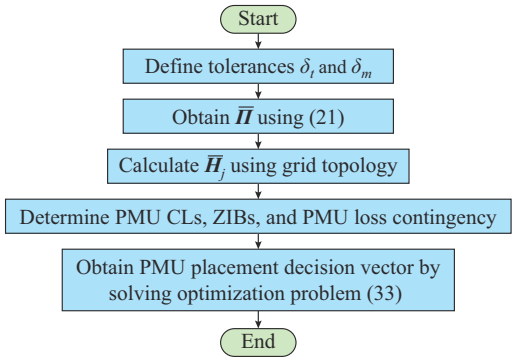

Fig. 1. Procedure for solving proposed OPP problem subject to different constraints.

The primary objective of the OPP problem is to minimize the number of PMUs while ensuring system observability [7], [12]-[14], [16], [17], [20], [29]. Therefore, the proposed OPP method considers constraints such as the PMU CLs, ZIBs, PMU loss contingency, SEE, and MSEEV while finding the PMU placement solution with the minimum number of PMUs. The method proposed in this paper is based on the non-Gaussian noise and the MLE and considers multiple constraints. The solution of (33) is useful for monitoring the system design to achieve a certain level of accuracy.

IV. Simulation Results

In this section, the performance of the proposed OPP method for different cases is evaluated in the IEEE 14-bus, 30-bus, and 118-bus systems. The numbers of ZIBs and branches for the above systems [47] are summarized in Table II. The placement solutions are obtained by using YALMIP with the CUTSDP solver [46] in MATLAB 2016a. The computer used to carry out the simulations is equipped with an Intel Core i7 central processing unit (CPU) running at 3.60 GHz with 8 GB of random access memory (RAM).

TABLE II
Numbers of ZIBs and Branches for Different Power Systems

System	Number of ZIBs	Location of ZIBs	Number of branches
IEEE 14-bus	1	7	20
IEEE 30-bus	6	6, 9, 22, 25, 27, 28	41
IEEE 118-bus	10	5, 9, 30, 37, 38, 63, 64, 68, 71, 81	186

The proposed OPP method is applicable to both Gaussian and non-Gaussian noise types when the probability density function (PDF) of the noise is known. As shown in (24), the proposed OPP method is identical to the OPP method based on the WLS estimator under the assumption of Gaussian measurement noise. Since the WLS-based OPP problem has been studied in [7], a non-Gaussian PDF is used in this study to model the measurement noise [49]:

$$f_i(\epsilon_i)=\begin{cases}\dfrac{96\%}{\sqrt{2\pi\sigma_i^2}}\exp\left(-\dfrac{\epsilon_i^2}{2\sigma_i^2}\right)+\dfrac{4\%}{20\sigma_i} & |\epsilon_i|\le 10\sigma_i\\ \dfrac{96\%}{\sqrt{2\pi\sigma_i^2}}\exp\left(-\dfrac{\epsilon_i^2}{2\sigma_i^2}\right) & \text{otherwise}\end{cases} \tag{45}$$

where $\sigma_i=0.005$. The standard deviation of the PMU measurement noise is usually between 0.0005 and 0.01 [50]. For simplicity, σ_i is set to be 0.005 in this study. A uniform distribution component can be used to model measurement outliers [34]. For the MLE, the maximum likelihood criterion is widely used to formulate the optimization problem, and the optimal parameters of the PDF can then be found to fit the data. The maximum likelihood criterion is implemented by minimizing $-\sum_{i=1}^{m}\ln(f_i(\epsilon_i(k)))$, where v_i and ξ_i are unknown. On the basis of the known data ϵ_i generated by (45), a t-distribution with parameters $v_i=3.10$ and $\xi_i=0.0035$ and a Gaussian distribution with $\sigma_i=0.006$ can be obtained to fit the histogram of measurement noise, as shown in Fig. 2. It is noted that the t-distribution can fit non-Gaussian noise more precisely than a Gaussian distribution. The simulation results obtained using the proposed OPP method under different operating conditions are presented below.

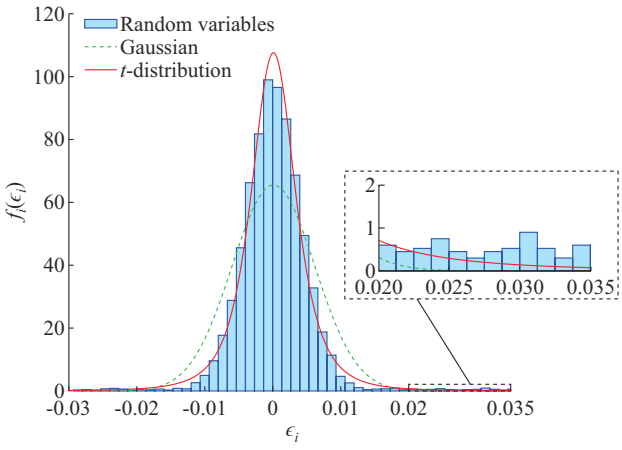

Fig. 2. Histogram of measurement noise approximated by a t-distribution with parameters $v_i=3.10$, $\xi_i=0.0035$, and a Gaussian distribution with $\sigma_i=0.006$.

A. Case Study Considering SEE and MSEEV

In this subsection, the effects of the SEE and MSEEV are considered in the IEEE 14-bus system. Note that the SEE or MSEEV for Gaussian noise and WLS are usually taken as the objective function in previous work [7], [19], [26], and the values of SEE or MSEEV are determined by the selec-

tion of a set of measurements. In this paper, different values of SEE δ_t and MSEEV δ_m are chosen to simulate different levels of SE accuracy for the WAMS. In practice, according to the historical SE results obtained from existing WAMS, the values of SEE and MSEEV should be further decreased to obtain a new PMU placement solution, and the relevant SEE is reduced, leading to an improvement in the SE accuracy. Note that more PMUs need to be placed or more measurements are needed if a smaller SEE is required. The objective of this simulation is to demonstrate whether the proposed OPP method can still find the optimal PMU placement solution when different SEE and MSEEV constraints are added for non-Gaussian noise and robust MLE. The simulation results in IEEE 14-bus system considering SEE or MSEEV constraints are given in Table III. For the "with SEE constraint only" case, the optimal PMU placement solutions are obtained, and the final SEE results are less than the predetermined SEE constraints. Moreover, the value of SEE is further decreased when the SEE constraints become more strict. The trade-off for a smaller SEE is to install more PMUs at certain buses or to place certain PMUs at different buses. For example, if the SEE constraint is set to be $\leq 180 \times 10^{-5}$, the PMUs are placed at Buses 2, 6, 7, and 9, which decreases the MSEEV and SEE results, i. e., 0.71×10^{-5} and 15.71×10^{-5}, respectively. This new placement result is better than the original placement vector [5], [10], [14], [16] because the SEE result is reduced from 27.92×10^{-5} to 15.71×10^{-5}. A minimum number of 11 PMUs is required to achieve an SEE that is less than 5.46×10^{-5}. In addition, the simulation results considering the SEE and MSEEV constraints are studied. When an SEE or MSEEV constraint becomes smaller, more PMUs are required, and the optimal PMU placement results are obtained. Even though an additional constraint is considered in the optimization problem, the MSEEV and SEE results are both within the given constraints.

TABLE III
SIMULATION RESULTS IN IEEE 14-BUS SYSTEM CONSIDERING SEE OR MSEEV CONSTRAINTS

With SEE constraint only					With SEE and MSEEV constraints						
SEE constraint (10^{-5})	Number of PMUs	Placement of PMUs	MSEEV result (10^{-5})	SEE result (10^{-5})	SEE constraint (10^{-5})	MSEEV constraint (10^{-5})	Number of PMUs	Placement of PMUs	MSEEV result (10^{-5})	SEE result (10^{-5})	Time (s)
≤ 1800.00	4	2, 7, 11, 13	1.22	27.92	≤ 1800.00	≤ 1.0	4	2, 6, 7, 9	0.71	15.72	0.6
≤ 180.00	4	2, 6, 7, 9	0.71	15.71		≤ 0.5	6	2, 6, 7, 9, 12, 14	0.44	10.40	0.9
≤ 11.00	6	1, 4, 6, 7, 9, 14	0.51	10.24	≤ 11.00	≤ 10.0	6	1, 4, 6, 7, 9, 14	0.51	10.22	0.8
						≤ 1.0	6	2, 4, 6, 7, 9, 14	0.51	10.01	1.0
≤ 7.29	9	2, 4, 6, 7, 8, 9, 11, 13, 14	0.30	6.61	≤ 7.29	≤ 1.0	9	2, 4, 6, 7, 8, 9, 11, 12, 14	0.26	6.61	0.7
≤ 5.46	11	2, 4, 5, 6, 7, 8, 9, 11, 12, 13, 14	0.21	5.37	≤ 5.46	≤ 1.0	11	2, 4, 5, 6, 7, 8, 9, 11, 12, 13, 14	0.21	5.36	0.7
						≤ 0.2	12	2, 4, 5, 6, 7, 8, 9, 10, 11, 12, 13, 14	0.19	4.93	0.4

B. Case Study Considering PMU CLs, ZIBs, Single PMU Loss Contingency, SEE, and MSEEV

The impacts of the ZIBs, single PMU loss contingency, and the available number of PMU channels on the traditional OPP solution have been examined [7], [16] - [18]. Here, the additional influences caused by the SEE and MSEEV in conjunction with the PMU CLs, ZIBs, and PMU loss contingency are evaluated. The IEEE 14-bus, 30-bus, and 118-bus systems are considered, and the simulation results are given in Table IV. Compared with the solutions given in [14], the inclusion of ZIBs reduces the required number of PMUs, and the number of ZIBs determines the reduction in the number of PMUs required. In addition, the PMU placement solution for the IEEE 14-bus system is the same as that in [14] when the SEE and MSEEV constraints are not considered. That is, nine PMUs are installed at Buses 2, 3, 5, 6, 7, 8, 9, 10, and 13. This verifies that the proposed OPP method is consistent and the obtained solutions are credible. The above placement solution is based on the assumption of Gaussian noise. When the *t*-distribution is considered and the SEE is more accurately calculated, the PMUs are installed at Buses 2, 4, 5, 6, 7, 8, 9, 11, and 13. The corresponding SEE result decreases from 6.74×10^{-5} to 6.62×10^{-5}. The number of installed PMUs remains the same. The SEE decreases to 5.92×10^{-5} when the number of PMUs increases to 10. In addition, given the predetermined SEE and MSEEV constraints, it is clear that a reduction in the available number of PMU channels leads to more PMUs being installed on certain buses. For example, the number of PMUs increases from 10 to 11 when the number of PMU channels changes from ∞ to 2. Similar improvements in the reduction in the SEE for the IEEE 30-bus and 118-bus systems can also be obtained, as summarized in Table IV. The execution time for solving the optimization problem considering multiple constraints is also given in Table IV. The execution time of the proposed OPP method increases with the size of the power system. Taking the IEEE 118-bus system as an example, the execution time of 6324.0 s has a similar order of magnitude as that in [7]. Therefore, the execution time overhead of the proposed OPP method is acceptable.

TABLE IV
SIMULATION RESULTS IN IEEE STANDARD SYSTEMS CONSIDERING PMU CLS, ZIBS, PMU LOSS CONTINGENCY, SEE, AND MSEEV

System	SEE constraint (10^{-5})	MSEEV constraint (10^{-5})	Number of PMUs	CL	Placement of PMUs	MSEEV result (10^{-5})	SEE result (10^{-5})	Time (s)
14-bus	$\leq\infty$	$\leq\infty$	9	∞	2, 3, 5, 6, 7, 8, 9, 10, 13	0.310	6.74	7.9
	$\leq$9.11	$\leq$1.0	9	∞	2, 4, 5, 6, 7, 8, 9, 11, 13	0.300	6.62	7.8
	$\leq$10.90	$\leq$0.5	10	∞	2, 4, 5, 6, 7, 8, 9, 11,13,14	0.280	5.92	15.3
	$\leq$10.90	$\leq$0.5	11	2	1, 2, 4, 6, 7, 9, 10, 11, 12, 13, 14	0.230	5.43	98.2
30-bus	$\leq\infty$	$\leq\infty$	21	∞	1, 2, 3, 5, 6, 8, 9, 10, 11, 12, 13, 15, 17, 19, 20, 22, 23, 25, 26, 27, 29	0.530	9.11	598.5
	$\leq$13.60	$\leq$5.0	21	∞	2, 3, 4, 6, 7, 9, 10, 11, 12, 13, 15, 17, 19, 20, 22, 24, 25, 26, 27, 28, 29	0.490	8.60	1080.6
	$\leq$13.60	$\leq$5.0	22	2	1, 2, 4, 5, 6, 9, 10, 11, 12, 13, 15, 16, 17, 18, 19, 21, 24, 25, 26, 27, 29, 30	0.290	7.86	3142.1
118-bus	$\leq\infty$	$\leq\infty$	66	∞	2, 3, 4, 6, 8, 9, 11, 12, 15, 16, 17, 19, 21, 22, 24, 25, 27, 28, 29, 32, 34, 35, 39, 40, 41, 43, 45, 46, 49, 50, 51, 53, 54, 56, 59, 62, 64, 66, 68, 70, 73, 75, 76, 77, 78, 80, 83, 85, 86, 87, 89, 91, 92, 94, 96,100, 101, 105, 106, 109, 110, 111, 112, 114, 116, 117	0.100	11.29	3651.7
	$\leq$10.12	$\leq$0.1	72	3	2, 3, 5, 7, 8, 10, 11, 12, 15, 17, 19, 20, 22, 23, 25, 27, 29, 30, 31, 32, 34, 36, 37, 38, 40, 42, 43, 45, 46, 49, 51, 53, 54, 56, 57, 59, 61, 62, 65, 66, 68, 69, 70, 71, 72, 75, 77, 78, 80, 81, 82, 83, 85, 86, 87, 89, 90, 92, 94, 96, 100, 101, 103, 105, 107, 109, 110, 111, 112, 115, 117, 117, 118	0.087	8.52	6324.0

C. Monitoring System Upgrades

Considering the number of available PMU channels and pre-existing SCADA measurements, the OPP method is important since there still exists a transition where both pre-existing SCADA and PMU measurements are utilized for the SE of the power system [51]. In reality, it is easy to obtain the SEE using the historical SE results. To increase the estimation accuracy of the monitoring system to a certain level, the SEE and MSEEV constraints can be added, and the proposed OPP method can provide the correct placement solution. In this example, a total of 84 measurements consisting of power flows and injected power for the IEEE 118-bus system are used [14]. The PMU placement solutions for different values of SEE are given in Table V. When the CL is 4, the values of SEE and MSEEV are 63.7×10^{-5} and 0.18×10^{-5}, respectively, and 24 PMUs are required. This verifies that the proposed OPP method is compatible with existing monitoring system upgrade. Once the desired SEE is achieved, the proposed OPP method can be used to determine the optimal PMU locations.

TABLE V
SIMULATION RESULTS FOR UPGRADED MONITORING SYSTEM IN IEEE 118-BUS SYSTEM

SEE constraint (10^{-5})	MSEEV constraint (10^{-5})	Number of PMUs	CL	Placement of PMUs	MSEEV result (10^{-5})	SEE result (10^{-5})	Time (s)
102.1	91.10	18	6	5, 9, 12, 19, 24, 32, 37, 49, 59, 61, 65, 68, 70, 80, 85, 92, 105, 110	1.45	95.1	611.4
63.7	0.18	24	4	5, 9, 12, 19, 24, 27, 30, 32, 37, 40, 49, 56, 59, 64, 68, 70, 80, 85, 86, 89, 95, 100, 105, 110	0.18	33.5	575.2

D. Practical 211-bus Distribution System in China

To further test the scalability of the proposed OPP method in a real distribution system, a system comprising 211 buses in China is considered [52]. There are many radial buses included in this 211-bus distribution system. If the PMU loss contingency is considered, each radial bus should be installed with one PMU, and the majority of distribution system buses should be installed with PMUs. Therefore, in this case, the constraints such as the PMU CLs, ZIBs, SEE, and MSEEV are considered, and the simulation results are given in Table VI. It is observed that the execution time is higher than those in Table IV since the number of PMU placement decision variables increases.

Even though the OPP methods based on topological observability theory can be applied to large-scale power systems by using an integer linear programming (ILP) method, they may not always ensure the numerical observability required for successful execution of SE [15]. Note that the numerical-observability-based OPP problem is usually formulated as an MISDP problem, and existing OPP methods based on numerical observability theory are applied to IEEE 14-bus, 57-bus, and 118-bus systems and 95-bus and 136-bus distribution systems [7], [14], [19], [21], [26], [29]. One possible drawback of SDP-based methods is their running time [53]. However, some solution methods such as the distributed SDP method [54] and solving constraint integer programs (SCIP) together with YALMIP [14] have been developed to reduce the running time.

Our main contribution is to form an MISDP problem linking OPP and SE of the power system and propose a new OPP method that considers the PMU CLs, ZIBs, PMU loss

contingency, SCADA measurements, SEE, and MSEEV. We will focus future work on a fast solution method for the MISDP problem.

TABLE VI
SIMULATION RESULTS IN 211-BUS DISTRIBUTION SYSTEM CONSIDERING PMU CLS, ZIBS, SEE, AND MSEEV

SEE constraint (10^{-5})	MSEEV constraint (10^{-5})	Number of PMUs	CL	Placement of PMUs	MSEEV result (10^{-5})	SEE result (10^{-5})	Time (s)
≤9.11	≤0.0183	106	3	1-6, 8, 10, 11, 12, 14, 15, 19, 23, 25, 27, 31, 32, 37, 41, 44, 46, 48, 52-57, 59-78, 80, 86, 88, 90, 92, 94, 98, 101, 109, 119, 121-126, 128-135, 137-149, 152, 153, 154, 156, 159, 161, 165, 169, 171, 174, 176, 179, 181, 184, 187, 192, 197, 209, 210	0.018	7.47	10213.2

V. CONCLUSION

A new OPP method is proposed for smart grids, where the PMU CLs, ZIBs, single PMU loss contingency, SCADA measurements, SEE, and MSEEV are considered. The SEE and MSEEV constraints are formulated as linear matrix inequality constraints using A- and G-optimal experimental criteria. The simulation results obtained from the IEEE 14-bus, 30-bus, and 118-bus systems and a real 211-bus distribution system in China verify the efficient performance of the proposed method. The proposed method is useful for designing and upgrading monitoring systems.

REFERENCES

[1] M. Xia, J. Sun, and Q. Chen, "Outlier reconstruction based distribution system state estimation using equivalent model of long short-term memory and Metropolis-Hastings sampling," *Journal of Modern Power Systems and Clean Energy*, vol. 10, no. 6, pp. 1625-1636, Nov. 2022.

[2] Y. Chen, H. Chen, Y. Jiao *et al*., "Data-driven robust state estimation through off-line learning and on-line matching," *Journal of Modern Power Systems and Clean Energy*, vol. 9, no. 4, pp. 897-909, Jul. 2021.

[3] P. Risbud, N. Gatsis, and A. Taha, "Multi-period power system state estimation with PMUs under GPS spoofing attacks," *Journal of Modern Power Systems and Clean Energy*, vol. 8, no. 4, pp. 597-606, Jul. 2020.

[4] S. Xu, H. Liu, and T. Bi, "Field PMU test and calibration method–part I: general framework and algorithms for PMU calibrator," *Journal of Modern Power Systems and Clean Energy*, vol. 10, no. 6, pp. 1507-1518, Nov. 2022.

[5] A. G. Phadke and T. Bi, "Phasor measurement units, WAMS, and their applications in protection and control of power systems," *Journal of Modern Power Systems and Clean Energy*, vol. 6, no. 4, pp. 619-629, Jul. 2018.

[6] Z. H. Rather, Z. Chen, P. Thøgersen *et al*., "Realistic approach for phasor measurement unit placement: consideration of practical hidden costs," *IEEE Transactions on Power Delivery*, vol. 30, no.1, pp. 3-15, Feb. 2015.

[7] T. C. Xygkis and G. N. Korres, "Optimized measurement allocation for power distribution systems using mixed integer SDP," *IEEE Transactions on Instrumentation and Measurement*, vol. 66, no.11, pp. 2967-2976, Nov. 2017.

[8] U.S. Department of Energy, Office of Electricity Delivery and Energy Reliability. (2014, Oct.). Factors affecting PMU installation costs. [Online]. Available: https://www. energy. gov/sites/prod/files/2016/10/f34/PMU-cost-study-final-101602141.pdf

[9] M. Ghamsari-Yazdel, M. Esmaili, F. Aminifar *et al*., "Incorporation of controlled islanding scenarios and complex substations in optimal WAMS design," *IEEE Transactions on Power Systems*, vol. 34, no. 5, pp. 3408-3416, Sept. 2019.

[10] A. Pal, A. K. S. Vullikanti, and S. S. Ravi, "A PMU placement scheme considering realistic costs and modern trends in relaying," *IEEE Transactions on Power Systems*, vol. 32, no. 1, pp. 552-561, Jan. 2017.

[11] A. Pal, C. Mishra, A. K. S. Vullikanti *et al*., "General optimal substation coverage algorithm for phasor measurement unit placement in practical systems," *IET Generation, Transmission & Distribution*, vol. 11, no. 2, pp. 347-353, Jan. 2017.

[12] M. K. Arpanahi, H. H. Alhelou, and P. Siano, "A novel multiobjective OPP for power system small signal stability assessment considering WAMS uncertainties," *IEEE Transactions on Industrial Informatics*, vol. 16, no. 5, pp. 3039-3050, May 2020.

[13] X. Zhu, M. H. F. Wen, V. O. K. Li *et al*., "Optimal PMU-communication link placement for smart grid wide-area measurement systems," *IEEE Transactions on Smart Grid*, vol. 10, no. 4, pp. 4446-4456, Jul. 2019.

[14] N. M. Manousakis and G. N. Korres, "Optimal allocation of phasor measurement units considering various contingencies and measurement redundancy," *IEEE Transactions on Instrumentation and Measurement*, vol. 69, no. 6, pp. 3403-3411, Jun. 2020.

[15] N. M. Manousakis and G. N. Korres, "Optimal PMU placement for numerical observability considering fixed channel capacity: a semidefinite programming approach," *IEEE Transactions on Power Systems*, vol. 31, no. 4, pp. 3328-3329, Jul. 2016.

[16] A. Bashian, M. Assili, and A. Anvari-Moghaddam, "A security-based observability method for optimal PMU-sensor placement in WAMS," *International Journal of Electrical Power & Energy Systems*, vol. 121, p. 106157, May 2020.

[17] N. M. Manousakis and G. N. Korres, "Optimal PMU arrangement considering limited channel capacity and transformer tap settings," *IET Generation, Transmission & Distribution*, vol. 14, no. 24, pp. 5984-5991, Nov. 2020.

[18] M. Picallo, A. Anta, and B. de Schutter, "Comparison of bounds for optimal PMU placement for state estimation in distribution grids," *IEEE Transactions on Power Systems*, vol. 34, no. 6, pp. 4837-4846, Nov. 2019.

[19] T. C. Xygkis, G. N. Korres, and N. M. Manousakis, "Fisher information-based meter placement in distribution grids via the D-optimal experimental design," *IEEE Transactions on Smart Grid*, vol. 9, no. 2, pp. 1452-1461, Mar. 2018.

[20] B. Appasani and D. K. Mohanta, "Co-optimal placement of PMUs and their communication infrastructure for minimization of propagation delay in the WAMS," *IEEE Transactions on Industrial Informatics*, vol. 14, no. 5, pp. 2120-2132, May 2018.

[21] N. M. Manousakis and G. N. Korres, "An advanced measurement placement method for power system observability using semidefinite programming," *IEEE Systems Journal*, vol. 12, no. 3, pp. 2601-2609, Sept. 2018.

[22] M. B. Mohammadi, R. H., and F. H. Fesharaki, "A new approach for optimal placement of PMUs and their required communication infrastructure in order to minimize the cost of the WAMS," *IEEE Transactions on Smart Grid*, vol. 7, no. 1, pp. 84-93, Jan. 2016.

[23] S. Almasabi and J. Mitra, "A fault-tolerance based approach to optimal PMU placement," *IEEE Transactions on Smart Grid*, vol. 10, no. 6, pp. 6070-6079, Nov. 2019.

[24] L. Sun, T. Chen, X. Chen *et al*., "Optimum placement of phasor measurement units in power systems," *IEEE Transactions on Instrumentation and Measurement*, vol. 68, no. 2, pp. 421-429, Feb. 2019.

[25] Y. Shi, H. D. Tuan, T. Q. Duong *et al*., "PMU placement optimization for efficient state estimation in smart grid," *IEEE Journal on Selected Areas in Communications*, vol. 38, no. 1, pp. 71-83, Jan. 2020.

[26] Y. Yao, X. Liu, and Z. Li, "Robust measurement placement for distribution system state estimation," *IEEE Transactions on Sustainable En-*

ergy, vol. 10, no. 1, pp. 364-374, Jan. 2019.
[27] S. Wang, J. Zhao, Z. Huang *et al*., "Assessing Gaussian assumption of PMU measurement error using field data," *IEEE Transactions on Power Delivery*, vol. 33, no. 6, pp. 3233-3236, Dec. 2018.
[28] J. A. D. Massignan, J. A. B. A. London, and V. Miranda, "Tracking power system state evolution with maximum-correntropy-based extended Kalman filter," *Journal of Modern Power Systems and Clean Energy*, vol. 8, no. 4, pp. 616-626, Jul. 2020.
[29] T. Chen, Y. Cao, X. Chen *et al*., "Optimal PMU placement approach for power systems considering non-gaussian measurement noise statistics," *International Journal of Electrical Power & Energy Systems*, vol. 126, p. 106577, Mar. 2021.
[30] T. Chen, H. Ren, X. Chen *et al*., "Optimal placement of pmu in distribution systems considering state estimation error," in *Proceedings of 2021 40th Chinese Control Conference (CCC)*, Shanghai, China, Jul. 2021, pp. 691-6926.
[31] M. Göl and A. Abur, "LAV based robust state estimation for systems measured by PMUs," *IEEE Transactions on Smart Grid*, vol. 5, no. 4, pp. 1808-1814, Jul. 2014.
[32] A. Abur and A. Gómez-Expósito, *Power System State Estimation: Theory and Implementation*. Boca Raton: CRC Press, 2004.
[33] Z. Shi, W. Yao, L. Zeng *et al*., "Convolutional neural network-based power system transient stability assessment and instability mode prediction," *Applied Energy*, vol. 263, p. 114586, Feb. 2020.
[34] T. Chen, L. Sun, K. Ling *et al*., "Robust power system state estimation using *t*-distribution noise model," *IEEE Systems Journal*, vol. 14, no. 1, pp. 771-781, Mar. 2020.
[35] S. Kotz and S. Nadarajah, *Multivariate t-distributions and Their Applications*. Cambridge: Cambridge University Press, 2004.
[36] F. Hampel, E. Ronchetti, P. Rousseeuw *et al*., *Robust Statistics: The Approach Based on Influence Functions*. Hoboken: Wiley, 2011.
[37] J. Zhao, M. Netto, and L. Mili, "A robust iterated extended Kalman filter for power system dynamic state estimation," *IEEE Transactions on Power Systems*, vol. 32, no. 4, pp. 3205-3216, Jul. 2017.
[38] S. Boyd and L. Vandenberghe, *Convex Optimization*. Cambridge: Cambridge University Press, 2004.
[39] X. Chen, F. Wei, S. Cao *et al*., "PMU placement for measurement redundancy distribution considering zero injection bus and contingencies," *IEEE Systems Journal*, vol. 14, no. 4, pp. 5396-5406, Dec. 2020.
[40] T. K. Maji and P. Acharjee, "Multiple solutions of optimal PMU placement using exponential binary PSO algorithm for smart grid applications," *IEEE Transactions on Industry Applications*, vol. 53, no. 3, pp. 2550-2559, May 2017.
[41] Y. F. Huang, S. Werner, J. Huang *et al*., "State estimation in electric power grids: meeting new challenges presented by the requirements of the future grid," *IEEE Signal Processing Magazine*, vol. 29, no. 5, pp. 33-43, Sept. 2012.
[42] Y. Chakhchoukh, H. Lei, and B. K. Johnson, "Diagnosis of outliers and cyber attacks in dynamic PMU-based power state estimation," *IEEE Transactions on Power Systems*, vol. 35, no. 2, pp. 1188-1197, Mar. 2020.
[43] J. P. Desai and V. H. Makwana, "Phasor measurement unit incorporated adaptive out-of-step protection of synchronous generator," *Journal of Modern Power Systems and Clean Energy*, vol. 9, no. 5, pp. 1032-1042, Sept. 2021.
[44] G. Cheng, Y. Lin, Y. Chen *et al*., "Adaptive state estimation for power systems measured by PMUs with unknown and time-varying error statistics," *IEEE Transactions on Power Systems*, vol. 36, no. 5, pp. 4482-4491, Sept. 2021.
[45] A. Bashian, M. Assili, and A. Anvari-Moghaddam, "Optimal placement of PMUs and related sensor-based communication infrastructures for full observability of distribution networks," in *Proceedings of 2020 IEEE PES General Meeting (PESGM)*, Montreal, Canada, Aug. 2020, pp. 1-5.
[46] J. Löfberg, "YALMIP: a toolbox for modeling and optimization in MATLAB," in *Proceedings of the CACSD Conference*, Taipei, China, Sept. 2004.
[47] K. G. Khajeh, E. Bashar, A. M. Rad *et al*., "Integrated model considering effects of zero injection buses and conventional measurements on optimal PMU placement," *IEEE Transactions on Smart Grid*, vol. 8, no. 2, pp. 1006-1013, Mar. 2017.
[48] YALMIP. (2021, Mar.). CUTSDP solver. [Online]. Available: https://yalmip.github.io/the-cutsdp-solver
[49] R. Baldick, K. Clements, Z. Pinjo-Dzigal *et al*., "Implementing nonquadratic objective functions for state estimation and bad data rejection," *IEEE Transactions on Power Systems*, vol. 12, no. 1, pp. 376-382, Feb. 1997.
[50] A. Gómez-Expósito, A. Abur, P. Rousseaux *et al*., "On the use of PMUs in power system state estimation," in *Proceedings of 17th Power Systems Computation Conference*, Stockholm, Sweden, Aug. 2011, pp. 1-26.
[51] W. Zheng and W. Wu, "An adaptive distributed quasi-Newton method for power system state estimation," *IEEE Transactions on Smart Grid*, vol. 10, no. 5, pp. 5114-5124, Sept. 2019.
[52] H. Su, C. Wang, P. Li *et al*., "Optimal placement of phasor measurement unit in distribution networks considering the changes in topology," *Applied Energy*, vol. 250, pp. 313-322, Sept. 2019.
[53] J. Park and S. Boyd, "A semidefinite programming method for integer convex quadratic minimization," *Optimum Letter*, vol. 12, pp. 499-518, Mar. 2018.
[54] S. K. Pakazad, A. Hansson, M. S. Andersen *et al*., "Distributed semidefinite programming with application to large-scale system analysis," *IEEE Transactions on Automatic Control*, vol. 63, no. 4, pp. 1045-1058, Apr. 2018.

Tengpeng Chen received the Ph. D. degree from the School of Electrical and Electronic Engineering, Nanyang Technological University, Singapore, in 2017. He is currently an Assistant Professor in the Department of Instrumental and Electrical Engineering, Xiamen University, Xiamen, China. His research interests include optimal PMU placement, distributed optimization algorithms with application in large-scale systems, power system state estimation, energy management for microgrid, and power system dynamics.

He Ren received the B. S. degree in electrical engineering from Sichuan University, Chengdu, China, in 2018. She is currently pursuing a master's degree in engineering from Xiamen University, Xiamen, China. Her research interest includes power system state estimation.

Yuhao Sun received the B. Eng. degree (first-class Honours) in electronics and communication engineering from Bristol University, Bristol, UK, in 2007, and the Ph. D. degree from the University of Cambridge, Cambridge, UK, in 2012. He held research positions with Cambridge University and the Singapore-Cambridge CREATE Research Centre, Cambridge, UK, respectively. He currently is the CEO of CTC Intelligence (Shenzhen) Technology Co., Ltd., Shenzhen, China, and Executive Director of SZ-HK International Advanced Technology Research Institute, Shenzhen, China. His research interests include distributed network monitoring system for power grid, precision monitoring instrument, and AI-based algorithm for power grid.

Markus Kraft received the academic degree "Diplom Technomathematiker" and the Ph. D. degree from the University of Kaiserslautern, Kaiserslautern, Germany, in 1992 and 1997, respectively. He is a Fellow of Churchill College Cambridge and a Professor with the Department of Chemical Engineering and Biotechnology, University of Cambridge, Cambridge, UK. He is the Director of CARES Ltd., the Singapore-Cambridge CREATE Research Centre, Cambridge, UK. His research interests include computational modeling and optimization targeted towards developing carbon abatement and emission reduction technologies.

Gehan A. J. Amaratunga received the B. Sc. degree (summa cum laude) in electronic engineering from Cardiff University, Cardiff, UK, in 1979, and the Ph. D. degree from the University of Cambridge, Cambridge, UK, in 1983. He has held academic and research positions with Southampton University, Southampton, UK, the University of Cambridge, Cambridge, UK, the University of Liverpool, Liverpool, UK, and Stanford University, Stanford, USA. Since 1998 he has been the 1966 Chair Professor of Engineering at the University of Cambridge and Fellow of Churchill College, Cambridge, UK. He was also the Chief of Research and Innovation at the Sri Lanka Institute of Nanotechnology (SLINTEC), Homagama, Sri Lanka (2011-2019) and Tan Chin Tuan Visiting Professor (2012-2014) and Visting Professor (2009-2018) with the Nanyang Technological University, Singapore. He is currently an Honorary Visting Professor at Peking University Shenzhen Graduate School, Shenzhen, China and Yunnan University, Kunming, China. He is a Fellow of the Royal Academy of Engineering, London, UK, Royal Society of Arts, London, UK, and the Institution of Engineering and Technology (formerly the IEE), London, UK. He is a recipient of the Royal Academy of Engineering Silver Medal (2007) for the successful commercialization of advanced research. His research interests include materials and technologies for electrical energy and power, which intersect electrical and electronic engineering with chemistry, physics, materials science, and information systems.